QRS Slopes for Detection and Characterization of Myocardial Ischemia

Esther Pueyo*, Leif Sörnmo, *Senior Member, IEEE*, and Pablo Laguna, *Senior Member, IEEE*

***Abstract*—In this study, the upward ($\mathcal{I}_{\mathrm{US}}$) and downward ($\mathcal{I}_{\mathrm{DS}}$) slopes of the QRS complex are proposed as indices for quantifying ischemia-induced electrocardiogram (ECG) changes. Using ECG recordings acquired before and during percutaneous transluminal coronary angioplasty (PTCA), it is found that the QRS slopes are considerably less steep during artery occlusion, in particular for $\mathcal{I}_{\mathrm{DS}}$. With respect to ischemia detection, the slope indices outperform the often used high-frequency index (defined as the root mean square (rms) of the bandpass-filtered QRS signal for the frequency band 150–250 Hz) as the mean relative factors of change are much larger for $\mathcal{I}_{\mathrm{US}}$ and $\mathcal{I}_{\mathrm{DS}}$ than for the high-frequency index (6.9 and 7.3 versus 3.7). The superior performance of the slope indices is equally valid when other frequency bands of the high-frequency index are investigated (the optimum one is found to be 125–175 Hz). Employing a simulation model in which the slopes of a template QRS are altered by different techniques, it is found that the slope changes observed during PTCA are mostly due to a widening of the QRS complex or a decrease of its amplitudes, but not a reduction of its high-frequency content or a combination of this and the previous effects. It is concluded that QRS slope information can be used as an adjunct to the conventional ST segment analysis in the monitoring of myocardial ischemia.**

***Index Terms*—Depolarization, high frequency, ischemia, percutaneous transluminal coronary angioplasty (PTCA), QRS complex.**

I. Introduction

MYOCARDIAL INFARCTION (MI) occurs when the blood supply to the myocardium is severely reduced or stops due to the blockage of one or more coronary arteries. If the blood supply is discontinued for several minutes, the cells suffer permanent injury and die (necrosis). Myocardial ischemia precedes infarction and is manifested by reduced blood flow to the heart, and may be caused by narrowing or occlusion of a coronary artery during a short period of time. Ischemia is sometimes accompanied with pain (angina pectoris) and sometimes without (silent ischemia), thus making its diagnosis more difficult.

During the first instants of acute coronary occlusion, ischemia is manifested in the electrocardiogram (ECG) by changes in the ventricular repolarization period (i.e., ST segment and T wave). Alterations during the ventricular depolarization (QRS complex) have traditionally been associated with the onset of the necrotic process. However, early animal studies demonstrated changes in QRS morphology due to slowing of intramyocardial conduction during ischemia [1]–[3]. Later on, similar results have been obtained in clinical studies with patients undergoing percutaneous transluminal coronary angioplasty (PTCA). During this procedure, a balloon is inserted and inflated inside a coronary artery to induce controlled ischemia, whereas, upon release, the blood flow to the cardiac cells is restored. Wagner *et al.* reported on changes in QRS amplitudes during PTCA [4]. Some changes occurred during the early part of inflation being secondary to ST-segment changes. However, primary changes occurred during the later part which were believed to reflect conduction delays. Since such changes disappeared after balloon deflation, they were associated with ischemia. In another study with patients undergoing elective PTCA in one of the major coronary arteries [5], the time course of ischemia was analyzed during both depolarization and repolarization. It was shown that QRS changes occur later in time than ST and T changes, indicating that more severe ischemia is required to cause depolarization changes.

In clinical practice, myocardial ischemia is usually diagnosed from changes in the ST segment, despite poor sensitivity and specificity. Other ECG indices derived from the Karhunen–Loève transform, applied to both depolarization and repolarization periods, have been proposed as additional tools for ischemia detection [6]. Although such indices seem to offer improved detection performance, they have not yet found their way into clinical routine. Recent studies have suggested that a decrease in high-frequency content (150–250 Hz) of the QRS complex is a better marker of ischemia than the traditional ST index [7]–[9]. However, the reduction in rms voltage of the high-frequency QRS components (HF–QRS) exhibits large interindividual variation, disqualifying this index for separation of subjects with and without coronary artery disease (CAD) [10] and subjects with and without previous MI [11]. The main clinical application of HF–QRS is thus restricted to the monitoring of ischemia in a given patient [12]–[14], unless a baseline HF–QRS value is available for the patient. In addition to the rms voltage, the high-frequency QRS components have

Manuscript received November 23, 2006; revised April 29, 2007. This work was part of the STAFF Studies Investigations and was supported in part by the Ministerio de Ciencia y Tecnología and FEDER under Project TEC2004-05263-C02-02, in part by the Diputación General de Aragón (DGA), Spain, through Grupos Consolidados GTC ref:T30, and in part by CIBER through ISCIII CIBER CB06/01/0062. *Asterisk indicates corresponding author.*

*E. Pueyo is with the Communications Technology Group (GTC) at the Aragón Institute for Engineering Research (I3A), and also with the Electronic Engineering and Communications Dept., Mar a de Luna 3, C/Carlos Saura 5, 4a, University of Zaragoza, Zaragoza 50015, Spain (e-mail: epueyo@unizar.es).

L. Sörnmo is with the Department of Electroscience, Signal Processing Group, Lund University, Lund SE-221 00, Sweden (e-mail: leif.sornmo@es.lth.se).

P. Laguna is with the Communications Technology Group (GTC) at the Aragón Institute for Engineering Research (I3A), and also with CIBER-BBN, University of Zaragoza, Zaragoza 50015, Spain (e-mail: laguna@unizar.es).

Color versions of one or more of the figures in this paper are available online at http://ieeexplore.ieee.org.

Digital Object Identifier 10.1109/TBME.2007.902228

been quantified by the presence of so-called reduced-amplitude zones (RAZ). Abboud *et al.* introduced an RAZ index which, in contrast to the rms voltage, was able to separate healthy subjects from CAD patients [10]. However, the electrophysiological factors determining the presence of RAZ remain to be explained, linking them to deterioration rather than to recovery of cardiac physiology [15], [16].

In the present study we analyze recordings acquired before and during prolonged PTCA for the purpose of assessing the temporal evolution of ischemic changes as the occlusion progresses. It is known that myocardial ischemia, in its advanced phase, modifies the electrophysiological properties of the ventricular cells by reducing the upstroke slope and the amplitude of the action potential, due to an increase in the potassium level of the extracellular space [1], [17], [18]. These alterations may be manifested as a widening of the QRS complex and a decrease in its amplitude. Accordingly, we hypothesize that the reduction in the upward and downward slopes of the QRS complex serve as measurements of ischemia-induced alterations. This approach avoids the problem of filter ringing, which smears the signal so that the nature of the localized HF–QRS features is masked. Furthermore, the proposed slope indices do not require signal averaging, but are computed directly from the ECG, thus constituting more robust indices. To further investigate this, we measure the QRS slopes and HF–QRS both before and during PTCA recordings and compare the abilities of the indices as well as some other traditional ECG indices, to detect ischemia-induced alterations.

II. Methods

A. Preprocessing

In the present work, preprocessing of the ECG signal includes QRS detection, selection of normal beats according to the method in [19], baseline drift attenuation via cubic spline interpolation, and wave delineation using a wavelet-based technique [20]. In the following, $x_i(n), n = 0, \ldots, N-1$ denotes the ith beat of a certain lead.

In contrast to measurements on a QRS slope, HF-QRS measurements require signal averaging to attain a sufficiently low noise level. In order to avoid smearing, beat alignment is performed prior to averaging using template cross-correlation. The template is built by averaging individual beats with the criterion that an incoming beat is included in the averaging only if the correlation coefficient between that beat and the existing template is above 0.97 [7], [21], [22]. Explicitly, the first QRS complex in the recording is used as a template beat. If the cross-correlation between the template and the second QRS exceeds 0.97 at the time instant for the best match, the two beats are averaged to produce a better template. If not, the first beat is discarded and the second one is used as a template beat. This procedure is repeated until ten consecutive beats have been found with a cross-correlation exceeding 0.97. The average of these ten beats defines the template to which subsequent beats are compared and accepted for averaging, provided that the cross-correlation exceeds 0.97.

For the control recording, ensemble averaging is applied to nonoverlapping blocks of 10 s, producing the averaged beat $\overline{x}_j(n)$, with j denoting the block index. For the PTCA recording, exponential averaging is employed so that changes can be tracked while still reducing the noise level. Ensemble averaging would not be appropriate for recordings where the ECG signal exhibits substantial morphological changes. The exponentially averaged beat $\overline{x}_i(n)$ is obtained by

$$\overline{x}_i(n) = (1 - \alpha_i)\overline{x}_{i-1}(n) + \alpha_i x_i(n) \tag{1}$$

where the weight α_i is inversely proportional to the noise level of $x_i(n)$. The noise level is related to the rms value of $x_i(n)$ bandpass filtered (150–250 Hz) in a 100-ms interval starting 100 ms after the QRS ends. An averaged beat $\overline{x}_j(n)$ is retained every 10 s for subsequent analysis from the beginning of occlusion. Leads for which an averaged beat cannot be obtained within the final 30 s of inflation (due to poor correlation) are discarded from further analysis.

The noise-level value is calculated for each averaged beat [7]. Two criteria are considered for rejection of noisy leads: either the noise level exceeds 0.75 μV at the end of occlusion or it differs from control to the end of occlusion by more than 0.35μV.

B. QRS Slope Indices ($\mathcal{I}_{\mathrm{US}}$ and $\mathcal{I}_{\mathrm{DS}}$)

Two indices are proposed to quantify ischemic QRS changes, measured in each beat of each lead of the preprocessed ECG, namely: 1) $\mathcal{I}_{\mathrm{US}}$: the upward slope of the QRS complex and 2) $\mathcal{I}_{\mathrm{DS}}$: the downward slope of the QRS complex.

A three-step process is applied to compute $\mathcal{I}_{\mathrm{US}}$ and $\mathcal{I}_{\mathrm{DS}}$. First, the time locations of the Q, R, and S peaks are determined by delineation, denoted by $n_{\mathrm{Q}}, n_{\mathrm{R}}$, and n_{S}, respectively. Beats for which n_{R} cannot be successfully determined are rejected from further analysis. Beats for which the delineator determines a valid n_{R}, but are unable to determine n_{Q} or n_{S}, a second search is performed. For the Q wave, the interval ranging from 2 ms after QRS onset until 2 ms before n_{R} is examined and the time instant associated with the lowest signal amplitude is identified as n_{Q}. Analogously, n_{S} is determined from the interval 2 ms after n_{R} until 2 ms prior to the QRS end. It should be noted that the determination of $n_{\mathrm{Q}}, n_{\mathrm{R}}$, and n_{S} is not critical since they just delimit the interval over which the slope is calculated.

The next step in the computation of $\mathcal{I}_{\mathrm{US}}$ and $\mathcal{I}_{\mathrm{DS}}$ is the determination of time instant n_{U} associated with the maximum slope of the ECG signal between n_{Q} and n_{R} (i.e., the global maxima of the derivative between n_{Q} and n_{R}) and, analogously, of n_{D}, leading to the minimum slope between n_{R} and n_{S}.

Finally, a pair of lines is fitted in the least squares sense to the ECG signal in windows of 15 ms centered around n_{U} and n_{D}, respectively; the resulting slopes are denoted as $\mathcal{I}_{\mathrm{US}}$ and $\mathcal{I}_{\mathrm{DS}}$ (Fig. 1).

C. QRS High-Frequency Indices ($\mathcal{I}_{\mathrm{HF}(f_0,f_1)}$)

The index $\mathcal{I}_{\mathrm{HF}(f_0,f_1)}$ is determined from the bandpass-filtered averaged beats, using a Butterworth filter with a passband between f_0 and f_1 Hz. In each case, the filtering required for the definition of $\mathcal{I}_{\mathrm{HF}(f_0,f_1)}$ is performed by processing the signal forwards and backwards to avoid phase distortion. The rms value of the bandpass-filtered QRS defines $\mathcal{I}_{\mathrm{HF}(f_0,f_1)}$, where QRS onset and end are identified from the unfiltered averaged

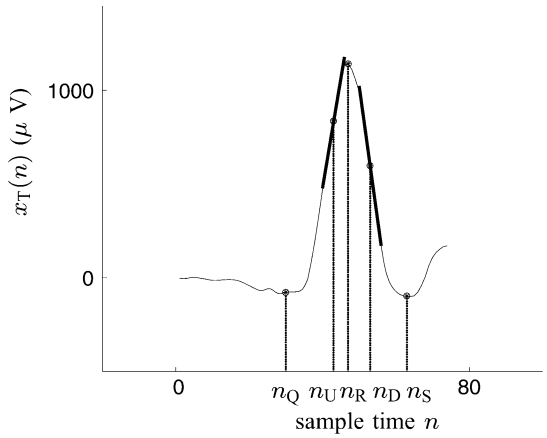

Fig. 1. Template of the simulation study and related upward and downward slopes $\mathcal{I}_{\rm US}$ and $\mathcal{I}_{\rm DS}$.

beat using the previously mentioned delineator [20]. The index $\mathcal{I}_{\rm HF(f_0,f_1)}$ is measured for different values of f_0, varying from 50 to 250 Hz, and f_1, varying from 100 to 300 Hz, both in steps of 25 Hz. The index $\mathcal{I}_{\rm HF(150,250)}$ is commonly employed in the literature [7], [13], [16].

D. Wave-Based ECG Indices

For comparison, traditional ECG indices, such as QRS duration (QRS$_d$) and S wave amplitude (S_a), are considered in this study. These indices are measured on each beat of the ECG for both the control and PTCA recordings.

E. Quantification of Ischemic Changes

The ability of a certain index $\mathcal{I}$ to track ischemic changes is characterized by the performance parameter $\mathcal{R}_\mathcal{I}$ [6]. This parameter is defined as the ratio between the change observed during PTCA, denoted as $\Delta_\mathcal{I}(t_j)$, and the normal fluctuations observed during the control recording as defined by the standard deviation $\sigma_\mathcal{I}$

$$\mathcal{R}_\mathcal{I}(t_j) = \frac{\Delta_\mathcal{I}(t_j)}{\sigma_\mathcal{I}}. \tag{2}$$

The numerator $\Delta_\mathcal{I}(t_j)$ is computed by fitting a linear polynomial to the values of $\mathcal{I}$ as measured from the onset of occlusion (i.e., $t = 0$) until $t = t_j$, where the time t_j is taken in increments of 10 s from $t = 0$. If γ_j denotes the slope of the fitted linear polynomial, the change $\Delta_\mathcal{I}(t_j)$ is calculated as the product $\gamma_j \cdot t_j$. This fitting strategy reduces the effect of outlier measurements on $\Delta_\mathcal{I}$. On the other hand, the denominator $\sigma_\mathcal{I}$ is computed as the standard deviation of $\mathcal{I}$ as measured in the control recording. In this study, any of the parameters in the set $\{\mathcal{I}_{\rm US}, \mathcal{I}_{\rm DS}, \mathcal{I}_{\rm HF(f_0,f_1)}, {\rm QRS}_d, S_a\}$ are used to define $\mathcal{R}_\mathcal{I}$.

III. ECG Data

The study population comprises 108 patients from the STAFF III database, receiving elective PTCA in one of the major coronary arteries at the Charleston Area Medical Center in West Virginia [6], [7]. Twenty-five patients were excluded from further analysis because they suffered from ventricular tachycardia, underwent an emergency procedure, or presented signal loss during acquisition. For the 83 patients (55 males and 28 females) in the study, the locations of the dilations were: left anterior descending artery (LAD) in 27 patients, right coronary artery (RCA) in 38 patients, and left circumflex artery (LCX) in 18 patients.

Nine standard leads (V1–V6, I, II, and III) were recorded using equipment from Siemens–Elema AB (Solna, Sweden), digitized at a sampling rate of 1 kHz with an amplitude resolution of 0.6 μV. The three augmented leads—aVR, aVL, and aVF—were readily generated from the limb leads so that the standard 12-lead ECG can be examined.

For each patient, two electrocardiograms are analyzed: 1) the control ECG, recorded immediately before occlusion and 2) the PTCA ECG recorded during occlusion. The duration of the control recording was around 5 min, whereas the PTCA ECG ranged from 1 min 30 s to 7 min 17 s, with a mean duration of 4 min 26 s. Note that the occlusion period was considerably longer than that of the usual PTCA procedure, since the treatment included a single prolonged occlusion rather than a series of brief occlusions.

IV. Simulated Data

Various tests with simulated QRS changes are designed with the objective to assess the performance of $\mathcal{I}_{\rm US}$ and $\mathcal{I}_{\rm DS}$ as well as $\mathcal{I}_{\rm HF(150,250)}$. The changes are generated by applying successive transformations to a template QRS, obtained by averaging beats of a 10-s period from one of the control recordings. This recording is chosen due to its high signal-to-noise ratio (SNR) and all beats of the selected 10-s period are highly correlated (> 0.97). The averaged QRS complex, displayed in Fig. 1, is used as a template $x_{\rm T}(n), n = 0, \ldots, N-1$ for the simulation tests. Taking the template QRS as the starting point, three different trials are proposed. Each test begins with a control period followed by a period of beat changes that mimic occlusion. The control period, which is common to all three tests, is defined by a succession of $L_{\rm c} = 100$ QRS complexes, where each complex $x_i(n)$ is obtained by adding the template $x_{\rm T}(n)$ to a variability signal $v_i(n)$

$$x_i(n) = x_{\rm T}(n) + v_i(n), \quad i = 1, \ldots, L_{\rm c}. \tag{3}$$

The recording used to generate the template is also used for deriving $v_i(n)$ through subtraction of the averaged QRS from each individual QRS. The resulting signal $v_i(n)$ is then curtailed to match the length of $x_{\rm T}(n)$. As a result, the variability introduced in the simulated complexes is similar to that observed in the control recording.

The transformation for each of the three proposed tests is described in the following:

Test 1: The simulated ECG is formed by gradually widening the template QRS such that the resulting series of Q to S peak durations follow a linear relationship. Explicitly, let $n_{\rm Q}, n_{\rm R}$, and $n_{\rm S}$ denote the time locations of Q, R, and S wave peaks, respectively, within the template $x_{\rm T}(n)$ (Fig. 1). The length of the upward QRS interval is denoted as $N_{\rm U}$ and the downward length as $N_{\rm D}$. The upward slope of each simulated QRS complex is generated by linear interpolation of $x_{\rm T}(n)$ between $n_{\rm Q}$ and $n_{\rm R}$ at $N_{\rm U} + i - 1$ equally spaced time instants; analogously, the downward slope is generated by linear interpolation of

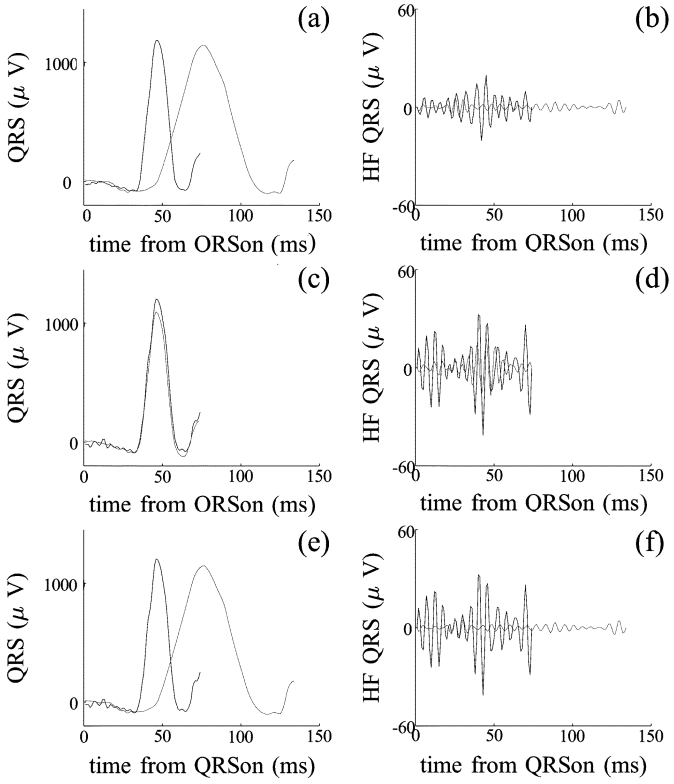

Fig. 2. In panels (a), (c), and (e), the first (dark gray) and last (light gray) simulated QRS complexes used in tests 1, 2, and 3, respectively, are shown. Panels (b), (d), and (f) contain their filtered (150–250 Hz) versions.

$x_{\mathrm{T}}(n)$ between n_{R} and n_{S} at $N_{\mathrm{D}}+i-1$ time instants. Finally, $v_i(n)$ is added to generate $x_i(n)$ so as to have variability during the transformation period. Since $x_{\mathrm{T}}(n)$ is gradually widened, the generated QRS complexes $x_i(n), i=1,\ldots,L_{\mathrm{t}}$ have increasing lengths N_i. Consequently, $v_i(n)$ needs to be adjusted to match N_i using the linear interpolation at N_i equally spaced time instants. Fig. 2(a) displays the first and last simulated QRS complexes, whereas Fig. 2(b) displays the bandpass-filtered versions.

Test 2: The simulated ECG is generated by adding high-frequency waveforms to the template QRS. Each waveform $s_i(n)$ is obtained by multiplying a source signal $s(n)$ by a factor β_i

$$s_i(n)=\beta_i\cdot s(n),\quad i=1,\ldots,L_{\mathrm{t}}. \tag{4}$$

The signal $s(n)$ is obtained by first subtracting the template to the last individual QRS of the 10-s segment from which the template was obtained. Next, the residual is filtered to generate $s(n)$ so that its frequency content is within 150 to 250 Hz. The factors β_i are chosen so that $\mathcal{I}_{\mathrm{HF}(150,250)}$ decreases in an inversely linear mode as i increases from 1 to L_{t}. The last factor $\beta_{L_{\mathrm{t}}}$ is forced to be zero so that the last simulated complex is identical to the template, while β_1 is selected in order to cause a relative decay in $\mathcal{I}_{\mathrm{HF}(150,250)}$ which is the same order as that imposed on the QRS slopes in test 1. In this test, the complexes $x_i(n)$ are defined as

$$x_i(n)=x_{\mathrm{T}}(n)+\beta_i\cdot s(n)+v_i(n) \tag{5}$$

where β_i is determined as described in the Appendix, and the series of $v_i(n)$ is identical to that used during control to introduce variability. The first and the last simulated complexes are presented in Fig. 2(c), together with their filtered versions [Fig. 2(d)].

Test 3: The simulated ECG is generated by combining tests 1 and 2 (i.e., accounting for both waveform widening and additional high-frequency waveform). Accordingly, the sequence $x_i(n), i=1,\ldots,L_{\mathrm{t}}$, comprises alterations of the same relative magnitude introduced both for $\mathcal{I}_{\mathrm{US}}$ and $\mathcal{I}_{\mathrm{DS}}$ (introduced by test 1) and for $\mathcal{I}_{\mathrm{HF}(150,250)}$ (introduced by test 2). Linear interpolation of $s(n)$ and $v_i(n)$ is required prior to filtering in order to match the length of the simulated QRS complexes. Fig. 2(e) presents the first and last QRS complexes of the transformation period and Fig. 2(f) presents their filtered versions.

In each test, a sequence of $L_{\mathrm{t}}=30$ QRS complexes is produced. Note that only 30 complexes are simulated in order to have physiologically plausible QRS patterns when applying the different transformations (the maximum simulated QRS duration is equal to 135 ms).

V. Results

A. Results on Real ECG Recordings

Out of the 996 examined leads (83 patients and 12 leads per patient), 800 were complied with the noise criteria (see Section II-A) and were accepted for subsequent analysis, thus representing 80.3%.

1) QRS Slope Alterations: Fig. 3 presents the absolute variations $\Delta_{\mathcal{I}_{\mathrm{US}}}$ and $\Delta_{\mathcal{I}_{\mathrm{DS}}}$, averaged over patients during 5-min occlusion, for leads V3 (in the transversal plane) and -aVR (in the frontal plane). The results obtained for these two leads are representative of the performance found in the other ten leads of the recordings. Note that each curve is based on fewer and fewer patients as time progresses due to different occlusion durations. It can be observed from Fig. 3 that both the upward and downward slopes become less steep as inflation progresses, manifested as decreasing negative values of $\Delta_{\mathcal{I}_{\mathrm{US}}}$ and increasing positive values of $\Delta_{\mathcal{I}_{\mathrm{DS}}}$. Measuring the mean$\pm$standard deviation of $\Delta_{\mathcal{I}_{\mathrm{US}}}$ and $\Delta_{\mathcal{I}_{\mathrm{DS}}}$ over patients along the occlusion time, it is found that their averaged values are $-3.0\pm9.9\,\mu$V/ms and 7.7$\pm$28.7 μV/ms, respectively, for lead V3. When calculated in lead -aVR, the corresponding values are $-1.6\pm5.8\,\mu$V/ms for $\Delta_{\mathcal{I}_{\mathrm{US}}}$ and 3.5$\pm$7.3 μV/ms for $\Delta_{\mathcal{I}_{\mathrm{DS}}}$.

In order to illustrate the results of Fig. 3, the upward and downward QRS slopes of one patient are displayed in Fig. 4 before and during PTCA. It can be observed that $\mathcal{I}_{\mathrm{US}}$, which is quite stable during the control, exhibits progressive reduction during inflation. Likewise, $\mathcal{I}_{\mathrm{DS}}$ presents a substantial variation from the onset of inflation, becoming gradually less steep.

2) Comparison of $\mathcal{I}_{\mathrm{US}}$, $\mathcal{I}_{\mathrm{DS}}$ and $\mathcal{I}_{\mathrm{HF}(f_0,f_1)}$: The index $\mathcal{I}_{\mathrm{HF}(f_0,f_1)}$ is evaluated in each lead of each analyzed recording, for the values of f_0 and f_1 given in Section II-C. The corresponding $\mathcal{R}_{\mathcal{I}_{\mathrm{HF}(f_0,f_1)}}$ is then calculated and averaged over patients during inflation, followed by averaging over leads. The maximum value attained over time is determined and displayed as a function of f_0 and f_1, see Fig. 5. The best frequency band for detecting ischemic changes is 125–175 Hz.

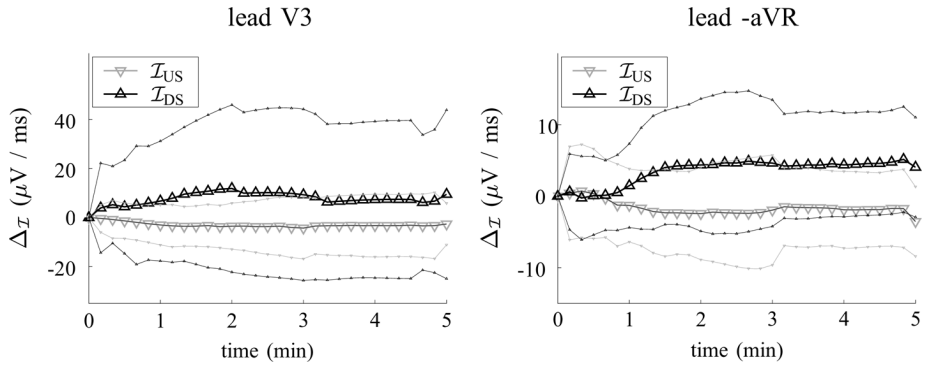

Fig. 3. Time course of absolute variations (mean $\pm$ standard deviation) for $\mathcal{I}_{\rm US}$ and $\mathcal{I}_{\rm DS}$ during 5-min occlusion.

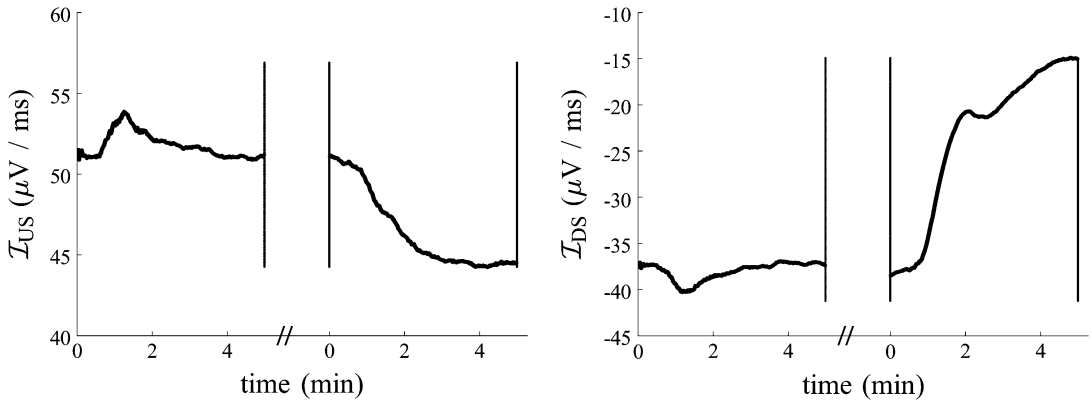

Fig. 4. Evolution of $\mathcal{I}_{\rm US}$ and $\mathcal{I}_{\rm DS}$ during control and PTCA measured in lead V6 for one particular patient of the study group. Vertical lines denote the end of the control recording, the start of the occlusion, and the end of the occlusion, respectively. Note the time gap (marked as//) between the two recordings.

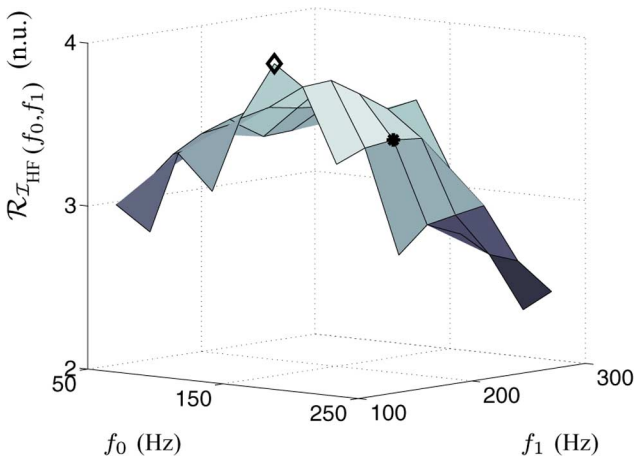

Fig. 5. $\mathcal{R}_{\mathcal{I}}$ for the index $\mathcal{I}_{{\rm HF}(f_0,f_1)}$. The maximum value is marked with $\diamond$, while the value associated with the standard $\mathcal{I}_{\rm HF(150,250)}$ is marked with $\bullet$.

The time course of changes, assessed by the absolute values of $\mathcal{R}_{\mathcal{I}}$ averaged over patients during 5 min of occlusion, is shown in Fig. 6 for $\mathcal{I}_{\rm US}, \mathcal{I}_{\rm DS}, \mathcal{I}_{\rm HF(150,250)}$ and $\mathcal{I}_{\rm HF(125,175)}$ in two different leads—V3 and -aVR. It is clear that $\mathcal{I}_{\rm HF(125,175)}$ yields better performance than $\mathcal{I}_{\rm HF(150,250)}$; however, the factor of change is far smaller than for $\mathcal{I}_{\rm US}$ and $\mathcal{I}_{\rm DS}$, especially for $\mathcal{I}_{\rm DS}$.

Measuring the mean$\pm$standard deviation of $\Delta_{\mathcal{I}_{\rm HF(150,250)}}$ over patients along the occlusion time, it is found that their averaged values are 0.17 ± 1.61 μV for lead V3 and $-0.18\pm1.55\mu$V for lead -aVR. It can be observed that the standard deviation calculated for $\mathcal{I}_{\rm HF(150,250)}$ is between eight and nine times its mean, while for $\mathcal{I}_{\rm US}$ and $\mathcal{I}_{\rm DS}$, it was only around three times.

3) Comparison of $\mathcal{I}_{\rm US}, \mathcal{I}_{\rm DS}$ and Wave-Based ECG Indices: The performance of $\mathcal{I}_{\rm US}$ and $\mathcal{I}_{\rm DS}$ is compared to QRS$_d$ and S_a, see Fig. 7. It can be observed that $\mathcal{I}_{\rm DS}$ and S_a exhibit relative variations of a higher magnitude than $\mathcal{I}_{\rm US}$ and QRS_d. The response of the four depolarization indices to the induced ischemia is not fast, but to the contrary, their $\mathcal{R}_{\mathcal{I}}$ values become more significant only from the second minute of occlusion.

B. Simulation Results

The evaluation of $\mathcal{I}_{\rm US}, \mathcal{I}_{\rm DS}$, and $\mathcal{I}_{\rm HF(150,250)}$ using test 1 is presented in Fig. 8(a)–(c). In Fig. 8(d), the absolute value of the $\mathcal{R}_{\mathcal{I}}$ parameter, calculated according to (2), is presented for the three indices. It can be observed from Fig. 8(a) and (b) that the QRS slopes decrease in absolute value, essentially following an inversely linear law. Also, $\mathcal{I}_{\rm HF(150,250)}$ decreases inversely linearly [Fig. 8(c)], although the extent of reduction in $\mathcal{R}_{\mathcal{I}_{\rm HF(150,250)}}$ is considerably smaller than for $\mathcal{R}_{\mathcal{I}_{\rm US}}$ and $\mathcal{R}_{\mathcal{I}_{\rm DS}}$ [Fig. 8(d)].

The results of test 2 are presented in Fig. 8(e)–(h) for $\mathcal{I}_{\rm US}, \mathcal{I}_{\rm DS}$, and $\mathcal{I}_{\rm HF(150,250)}$. It can be observed that $\mathcal{I}_{\rm HF(150,250)}$

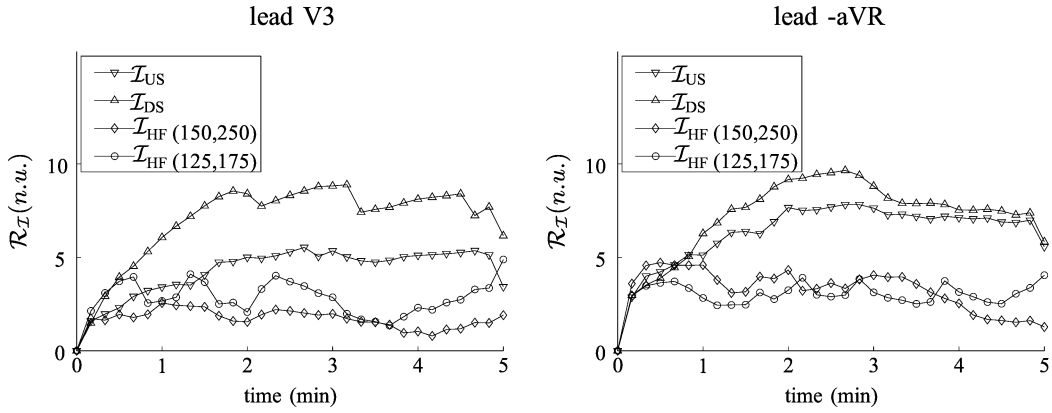

Fig. 6. Temporal evolution of averaged $\mathcal{R}_{\mathcal{I}}$ absolute values, for indices $\mathcal{I} = \mathcal{I}_{\mathrm{US}}, \mathcal{I}_{\mathrm{DS}}, \mathcal{I}_{\mathrm{HF}(150,250)}$, and $\mathcal{I}_{\mathrm{HF}(125,175)}$.

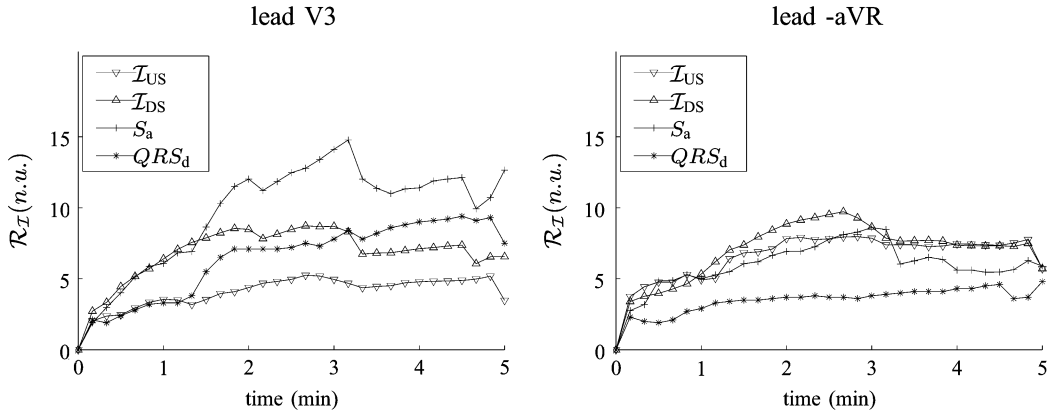

Fig. 7. Temporal evolution of averaged $\mathcal{R}_{\mathcal{I}}$ absolute values, for indices $\mathcal{I} = \mathcal{I}_{\mathrm{US}}, \mathcal{I}_{\mathrm{DS}}, S_a$, and QRS_d.

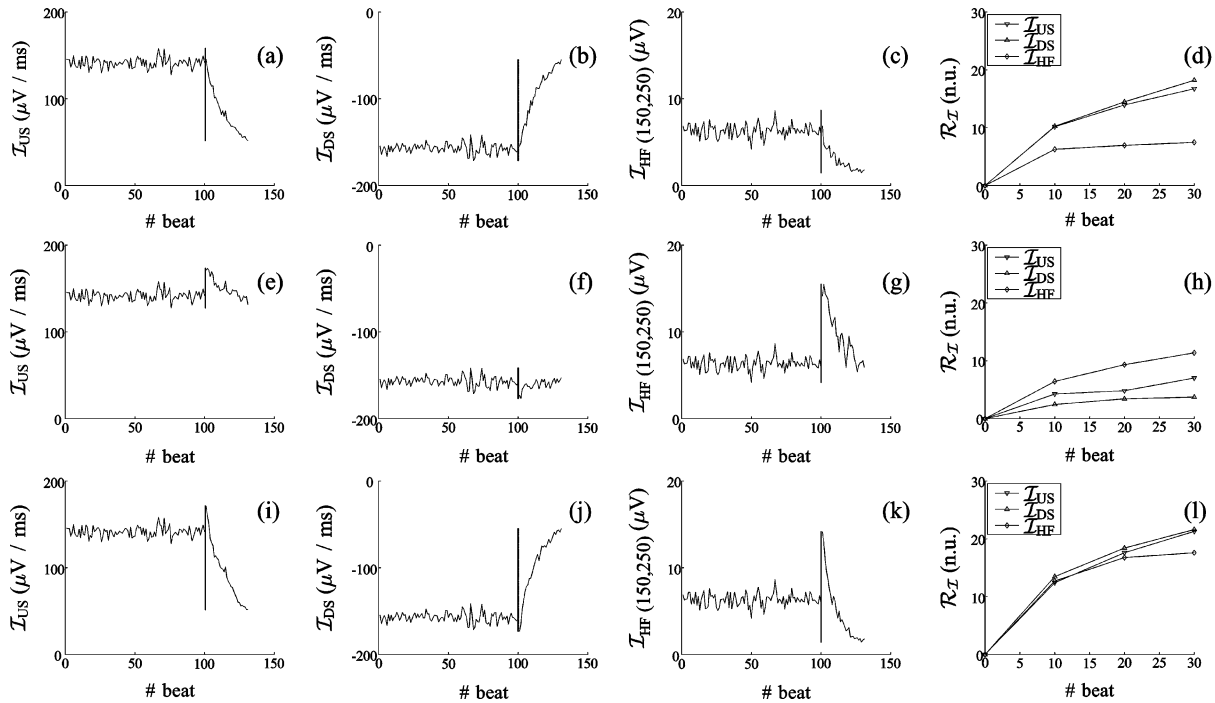

Fig. 8. Results of simulation test 1 are shown in the top row. Panels (a), (b), and (c) contain the evaluation of $\mathcal{I}_{\mathrm{US}}, \mathcal{I}_{\mathrm{DS}}$, and $\mathcal{I}_{\mathrm{HF}(150,250)}$, while panel (d) presents the corresponding absolute $\mathcal{R}_{\mathcal{I}}$ values. Analogously, results of simulation test 2 are shown in the middle row (panels (e), (f), (g), and (h)), and the results of simulation test 3 in the bottom row [panels (i), (j), (k), and (l)].

decreases in an inversely linear way and its relative factor of change is slightly smaller than those of the slopes in test 1 (the reason why it is not the same is that the effect of adding the signals $v_i(n)$ is not accounted for in the derivation of β_i). The decay of the QRS slopes in absolute value is inferior to that of $\mathcal{I}_{\mathrm{HF}(150,250)}$, although the upward slope is more influenced by the induced alteration than the downward one.

Fig. 8(i)–(k) shows the evolution of $\mathcal{I}_{\mathrm{US}}$, $\mathcal{I}_{\mathrm{DS}}$, and $\mathcal{I}_{\mathrm{HF}(150,250)}$ during the control and the transformation periods of test 3. In Fig. 8(l), the absolute value of $\mathcal{R}_{\mathcal{I}}$ is presented for the three indices, establishing that $\mathcal{R}_{\mathcal{I}}$ is larger for $\mathcal{I}_{\mathrm{US}}$ and $\mathcal{I}_{\mathrm{DS}}$ than for $\mathcal{I}_{\mathrm{HF}(150,250)}$. Besides, it can be observed that the three indices present relative variations of magnitude higher than those found in tests 1 and 2 due to the combination of the effects induced by both tests. Note that the jumps in the separation of the represented index values during the control and the transformation period in Fig. 8(e)–(g) and Fig. 8(i)–(k) do not affect the evaluation of the ratio that defines $\mathcal{R}_{\mathcal{I}}$, since the numerator and the denominator are computed separately for each of the two periods.

VI. Discussion

In this study, two new indices are proposed to quantify ischemic changes during depolarization, describing the upward and downward slopes of the QRS complex. The more commonly used $\mathcal{I}_{\mathrm{HF}(150,250)}$ has been found to decrease in patients with IHD when compared to healthy individuals [21]. Trägårdh *et al.* attributed their findings to the fact that IHD causes structural changes in the myocardium that give rise to abnormal impulse propagation in the heart. A decrease in HF–QRS was also reported during acute myocardial ischemia [7], and related to the slowing of conduction velocity in the ischemic region. In animal studies, $\mathcal{I}_{\mathrm{HF}(150,250)}$ has been proposed as a marker of abnormal local conduction caused by the infusion of sodium channel blockers [23]. An experimental investigation with a ventricular model was studied for the purpose of explaining the physiological mechanisms that provoke the changes in $\mathcal{I}_{\mathrm{HF}(150,250)}$ for the aforementioned heart diseases [24]. Using that model, Abboud *et al.* corroborated that regional reduction of conduction velocity generates changes in HF–QRS similar to those observed in [7], [21], and [23].

Despite the fact that $\mathcal{I}_{\mathrm{HF}(150,250)}$ is reduced in IHD patients, when compared to healthy subjects, no significant difference in $\mathcal{I}_{\mathrm{HF}(150,250)}$ was found between individuals with and without CAD [10]; this result is explained by the large interindividual variation of $\mathcal{I}_{\mathrm{HF}(150,250)}$. On the other hand, the interrecording variation from the same individual is very low [12], [22] and, consequently, the use of $\mathcal{I}_{\mathrm{HF}(150,250)}$ is suitable for monitoring ischemia over time. This limitation is most likely due to the underlying physiological phenomenon, but perhaps also to smearing caused by bandpass filtering of the QRS complex.

Attempts have been made to quantify adverse QRS changes in the ECG. In [12], the peak-to-peak QRS amplitude and $\mathcal{I}_{\mathrm{HF}(150,250)}$ were measured in signal-averaged ECG leads from patients with IHD. It was found that the spatial variation of the HF components depends on factors other than the peak-to-peak QRS amplitude. In a theoretical study, a model of the cardiac cell was developed and ischemia was simulated [17]. It was found that during the advanced phase of ischemia, the QRS complex became considerably wider while, at the same time, its amplitude decreased. In [25], a preliminary report was published that assessed QRS slopes changes for characterization of myocardial ischemia. During PTCA, it was shown that both slopes decreased in absolute value as ischemia progressed, the largest reduction occurred during the second minute of occlusion. In [26], the first major deflection of the QRS complex was evaluated in patients undergoing percutaneous coronary intervention. Although the sensitivity of that method for ischemia detection was found to be considerably greater than that of the conventional ECG measures, its low specificity limits its clinical usefulness. Nevertheless, it should be noticed that in [26], the duration of the occlusion recordings is blinded to the study, but its mean is 1.4 min. According to the results found in our study, we believe that longer occlusions provoking a more severe ischemia would lead to more visible depolarization changes.

Based on the observations in [17] and the results of [12], a simulation study is proposed in this work to find out how the broadening of QRS duration and addition of high-frequency signals (150–250 Hz) influence the performance of $\mathcal{I}_{\mathrm{US}}, \mathcal{I}_{\mathrm{DS}}$, and $\mathcal{I}_{\mathrm{HF}(150,250)}$. It is demonstrated that all simulated conditions clearly alter the three indices. Also, an extra test (not presented in this study) was performed in which a simulated sequence of QRS complexes was obtained as a result of shortening the peak-to-peak amplitudes of the template QRS in an inversely linear manner, yielding results very similar to those of test 1 in terms of relative changes. Consequently, it can be emphasized that the transformations of test 1 and the extra test, implying a reduction of the QRS slopes, also cause a decrease in the high-frequency (HF) components. Conversely, the alteration of the HF components in test 2 also modifies the two QRS slopes. Thus, it is clear that part of the information provided by $\mathcal{I}_{\mathrm{HF}(150,250)}$ is common to that of $\mathcal{I}_{\mathrm{US}}$ and $\mathcal{I}_{\mathrm{DS}}$, although not necessarily representing the same physiological phenomenon. When the control situation is taken into account in the simulation, the relative changes of $\mathcal{I}_{\mathrm{US}}$ and $\mathcal{I}_{\mathrm{DS}}$ are found to be larger than those of $\mathcal{I}_{\mathrm{HF}(150,250)}$.

In this study, $\mathcal{I}_{\mathrm{US}}$ and $\mathcal{I}_{\mathrm{DS}}$ were evaluated on ECGs obtained from patients before and during PTCA. As hypothesized, it is shown that the QRS slopes become less steep during induced ischemia, especially for $\mathcal{I}_{\mathrm{DS}}$. The observation that the downward QRS slope exhibits substantial reduction during the course of ischemia is consistent with the findings reported in [5]. In that work, the amplitudes of Q, R, and S waves were assessed using the present database. It was concluded that the S-wave amplitude exhibited the largest change with performance superior to that of ST60 in certain leads. A justification for the results of our study has to do with the fact that, after some minutes of balloon occlusion, high-grade ischemia makes the ventricular activation time increase, indicating slowing conduction velocity. Thus, as time progresses, some action potentials start to be delayed, while others have already completed depolarization. This delay has a strong effect on the downward stroke of the QRS complex, which reduces its amplitude and its slope considerably. In this respect, Fig. 7 shows that the variations during PTCA relative to the normal fluctuations during control

are more manifested in terms of amplitude for lead V3, while they are more noticeable in terms of slope for lead -aVR.

This study shows that $\mathcal{I}_{\rm US}$ and $\mathcal{I}_{\rm DS}$ are better in detecting ischemia than $\mathcal{I}_{\rm HF(150,250)}$. In fact, Fig. 6 shows that the factor of change associated with $\mathcal{I}_{\rm DS}$ is more than twice as large as that of $\mathcal{I}_{\rm HF(150,250)}$. Comparing these results with the ones obtained from the simulation tests (Fig. 8(d), (h), and (l)), it is noted that the results found in ECG recordings are similar to those obtained in the simulation test 1, when expressed by the ratio $\mathcal{R}_{\mathcal{I}_{\rm DS}}/\mathcal{R}_{\mathcal{I}_{\rm HF(150,250)}}$, but not to those of tests 2 and 3. Consequently, it can be concluded that slope changes observed during PTCA are most likely due to a widening of the QRS complex (or a decrease in the QRS amplitudes) than to a reduction in the high-frequency (150–250 Hz) content of the QRS complex exclusively or a combination of both. With respect to QRS duration during PTCA, it can be seen from Fig. 7 that the factor of change $\mathcal{R}_{QRS_d}$ reaches a maximum value between 4 and 8, depending on the lead. According to our results, the ability of $\mathcal{I}_{\rm DS}$ to reflect ischemic changes is, in mean between leads, superior to that of QRS$_d$. This can be explained because $\mathcal{I}_{\rm DS}$ is also altered by QRS amplitude changes and because the variability during control is proportionally higher for QRS$_d$ than for $\mathcal{I}_{\rm DS}$ (probably because measurement uncertainty is reduced in slope computations). Finally, although the slope indices have not been compared with the ST level in the present work, previous studies performed on the same database described in Section III have shown that acute coronary occlusion is detected with higher sensitivity using $\mathcal{I}_{\rm HF(150,250)}$ than with the conventional ST deviation [7], [27]. Consequently, we conclude that $\mathcal{I}_{\rm US}$ and $\mathcal{I}_{\rm DS}$ provide information complementary to that of ST.

The performance associated with frequency bands different from the standard one was also studied. The results indicate that a considerably lower frequency band (i.e., 125–175 Hz), is more sensitive to ischemia, although it is noted from Fig. 5 that $\mathcal{R}_{\mathcal{I}_{\rm HF(f_0,f_1)}}$ is quite flat around the optimal (f_0, f_1). Nonetheless, the relative magnitude of change associated with any of the tested high-frequency indices is, at best, half of that of $\mathcal{I}_{\rm DS}$. Moreover, the slope indices have the dramatic advantage of being easier to compute since they do not require signal averaging but are obtained directly from the ECG. Although further clinical studies are needed to evaluate the full significance of $\mathcal{I}_{\rm DS}$, the present study has demonstrated that this index has considerable potential for ischemia detection and characterization.

VII. Conclusion

The QRS slopes promise to be a sensitive method for quantifying ischemic variations, particularly the downward slope. A comparison with high-frequency indices shows that the slope indices have ischemia-induced alterations of twice the magnitude than that for high-frequency analysis. Furthermore, the slope indices provide more robust measurements since they do not require signal averaging but can be applied directly to the raw ECG. We suggest that the QRS slopes can be used for monitoring ischemia over time, while their use for separation of individuals with and without CAD needs to be tested in future studies.

Appendix

The factors β_i in test 2 of Section IV are defined as follows. Let us denote

$$K_1 = \sum_{n=0}^{N-1} y_{\rm T}^2(n),$$
$$K_2 = \sum_{n=0}^{N-1} s^2(n),$$
$$K = \sum_{n=0}^{N-1} y_{\rm T}(n)s(n) \tag{6}$$

where $y_{\rm T}(n)$ denotes the bandpass filtered ($f_0 - f_1$ Hz) version of the template $x_{\rm T}(n)$ and $s(n)$ the source signal. The index $\mathcal{I}_{\rm HF(f_0,f_1)}$, based on $x_i(n)$ (prior to the addition of the noise signals $v_i(n)$)s, is equal to a value of $\sqrt{(K_1 + \beta_i^2 K_2 + 2\beta_i K)/N}$. Since an inversely linear decay needs to be established for the series of $\mathcal{I}_{\rm HF(f_0,f_1)}$ values, the following expression must hold:

$$\sqrt{\frac{K_1 + \beta_i^2 K_2 + 2\beta_i K}{N}} = \frac{1}{ai + b}, \qquad i = 1, \ldots, L_{\rm t} \tag{7}$$

for certain real numbers a and b, with $a < 0$ determined from the imposition that

$$\beta_{L_{\rm t}} = 0 \tag{8}$$
$$\sqrt{\frac{K_1 + \beta_1^2 K_2 + 2\beta_1 K}{N}} - \sqrt{\frac{K_1}{N}} = \mu \tag{9}$$

where $\mu = \lambda \cdot \sigma_{\mathcal{I}_{\rm HF(f_0,f_1)}}$, λ is the factor $\mathcal{R}_{\mathcal{I}_{\rm US}}$ at the final evaluated time of test 1 (if no additive signals $v_i(n)$ were incorporated) and $\sigma_{\mathcal{I}_{\rm HF(f_0,f_1)}}$ the standard deviation of $\mathcal{I}_{\rm HF(f_0,f_1)}$ in the control period. In this way, the relative magnitude of change attained by $\mathcal{I}_{\rm HF(f_0,f_1)}$ in test 2 coincides with that of the upward slope in test 1.

In order to solve for β_i, $i = 1, \ldots, L_{\rm t}$, the parameters a and b are first determined from the conditions

$$a = \frac{1}{L_{\rm t} - 1}\left(\sqrt{\frac{N}{K_1}} - F\right), \quad b = F - a \tag{10}$$

with

$$F = \frac{\sqrt{N}}{\sqrt{K_1} + \mu\sqrt{N}}. \tag{11}$$

This, in turn, leads to the consideration, from (7), of the second-order polynomials $P_i(\beta), i = 1, \ldots, L_{\rm t}$, defined as

$$P_i(\beta) = A\beta^2 + B\beta + C_i, \quad i = 1, \ldots, L_{\rm t} \tag{12}$$

with

$$A = K_2, \quad B = 2K, \quad C_i = K_1 - \frac{N}{(ai + b)^2} \tag{13}$$

and a and b as the ones derived in (10). It can be readily checked that each polynomial $P_i(\beta)$ has a unique positive root identified as β_i. Moreover, it is also corroborated that such roots β_i satisfy

$$0 \le \beta_i < \beta_{i-1}, \quad i = 2, \ldots, L_{\rm t}. \tag{14}$$

REFERENCES

[1] R. P. Holland and H. Brooks, "The QRS complex during myocardial ischemia: An experimental analysis in the porcine heart," *J. Clin. Invest.*, vol. 57, pp. 541–550, 1976.

[2] R. L. Hamlin, F. S. Pipers, H. K. Hellerstein, and C. R. Smith, "Alterations in the QRS during ischemia of the left ventricular free-wall in goats," *J. Electrocardiol.*, vol. 2, pp. 223–228, 1969.

[3] R. L. Hamlin, F. S. Pipers, H. K. Hellerstein, and C. R. Smith, "QRS alterations immediately following production of left ventricular free-wall ischemia in dogs," *4m. J. Physiol.*, vol. 215, pp. 1032–1040, 1968.

[4] N. B. Wagner, D. C. Sevilla, M. W. Krucoff, K. L. Lee, K. S. Pieper, K. K. Kent, R. K. Bottner, R. H. Selvester, and G. S. Wagner, "Transient alterations of the QRS complex and ST segment during percutaneous transluminal balloon angioplasty of the left anterior descending coronary artery," *Amer. J. Cardiol.*, vol. 62, pp. 1038–1042, 1988.

[5] E. Pueyo, J. García, G. Wagner, R. Bailón, L. Sörnmo, and P. Laguna, "Time course of ECG depolarization and repolarization changes during ischemia in PTCA recordings," *Methods Inf. Med.*, vol. 43, pp. 43–46, 2004.

[6] J. García, G. Wagner, L. Sörnmo, S. Olmos, P. Lander, and P. Laguna, "Temporal evolution of traditional versus transformed ECG-based indexes in patients with induced myocardial ischemia," *J. Electrocardiol.*, vol. 33, pp. 37–47, 2000.

[7] J. Pettersson, O. Pahlm, E. Cairo, L. Edenbrandt, M. Ringborn, L. Sörnmo, S. G. Warren, and G. S. Wagner, "Changes in high-frequency QRS components are more sensitive than ST-segment deviation for detecting acute coronary artery occlusion," *J. Amer. Coll. Cardiol.*, vol. 36, pp. 1827–1834, 2000.

[8] S. Abboud, R. J. Cohen, A. Selwyn, P. Ganz, D. Sadeh, and P. L. Friedman, "Detection of transient myocardial ischemia by computer analysis of standard and signal-averaged high frequency electrocardiograms in patients undergoing percutaneous transluminal coronary angioplasty," *Circulation*, vol. 76, no. 3, pp. 585–596, 1987.

[9] A. Beker, A. Pinchas, J. Erel, and S. Abboud, "Analysis of high frequency QRS potential during exercise testing in patients with coronary artery disease and in healthy subjects," *Pacing Clin. Electrophysiol.*, vol. 19, no. 12, pp. 2040–2050, 1996.

[10] S. Abboud, B. Belhassen, H. I. Miller, D. Sadeh, and S. Laniado, "High frequency electrocardiography using an advanced method of signal averaging for non-invasive detection of coronary artery disease in patients with normal conventional electrocardiogram," *J. Electrocardiol.*, vol. 19, no. 4, pp. 371–380, 1986.

[11] M. Ringborn, O. Pahlm, G. S. Wagner, S. G. Warren, and J. Pettersson, "The absence of high-frequency QRS changes in the presence of standard electrocardiographic QRS changes of old myocardial infarction," *Amer. Heart J.*, vol. 141, no. 4, pp. 573–579, 2001.

[12] J. Pettersson, E. Cairo, L. Edenbrandt, C. Maynard, O. Pahlm, M. Ringborn, L. Sommo, S. G. Warren, and G. S. Wagner, "Spatial, individual, and temporal variation of the high-frequency QRS amplitudes in the 12 standard electrocardiographic leads," *Amer. Heart J.*, vol. 139, pp. 352–358, 2000.

[13] S. Abboud, "High-frequency electrocardiogram analysis of the entire QRS in the diagnosis and assessment of coronary artery disease," *Prog. Cardiovasc. Dis.*, vol. 35, no. 5, pp. 311–328, 1993.

[14] T. Aversano, B. Rudikoff, A. Washington, S. Traill, V. Coombs, and J. Raqueno, "High frequency QRS electrocardiography in the detection of reperfusion following thrombolytic therapy," *Clin. Cardiol.*, vol. 17, no. 4, pp. 175–182, 1994.

[15] S. Abboud and S. Zlochiver, "High-frequency QRS electrocardiogram for diagnosing and monitoring ischemic heart disease," *J. Electrocardiol*, vol. 39, pp. 82–86, 2006.

[16] T. T. Schlegel, W. B. Kulecz, J. L. DePalma, A. Feiveson, J. Wilson, M. A. Rahman, and M. W. Bungo, "Real-time 12- lead high-frequency QRS electrocardiography for enhanced detection of myocardial ischemia and coronary artery disease," *Proc. Mayo Clin.*, vol. 79, no. 3, pp. 339–350, 2004.

[17] A. Cimponeriu, C. F. Starmer, and A. Bezerianos, "A theoretical analysis of acute ischemia and infarction using ECG reconstruction on a 2-D model of myocardium," *IEEE Trans. Biomed. Eng.*, vol. 48, no. 1, pp. 41–54, Jan. 2001.

[18] M. Vandyck-Acquah and P. Schweitzer, "Electrocardiographic background," in *Dynam. Electrocardiography*, M. Malik and A. Camm, Eds. Oxford, U.K.: Blackwell Future, 2004, pp. 217–232.

[19] G. B. Moody and R. G. Mark, "Developement and evaluation of a 2-lead ECG analysis program," in *Proc. Computers Cardiology*. New York: IEEE Comput. Soc. Press, 1982, pp. 39–44.

[20] J. P. Martinez, R. Almeida, S. Olmos, A. P. Rocha, and P. Laguna, "A wavelet-based ECG delineator: Evaluation on standard databases," *IEEE Trans. Biomed. Eng.*, vol. 51, no. 4, pp. 570–581, Apr. 2004.

[21] E. Trägårdh, O. Pahlm, G. S. Wagner, and J. Pettersson, "Reduced high-frequency QRS components in patients with ischemic heart disease compared to normal subjects," *J. Electrocardiol.*, vol. 37, pp. 157–162, 2004.

[22] N. J. Batford, A. H. Feiveson, and T. T. Schlegel, "Month-to-month and year-to-year reproducibility of high frequency QRS ECG signals," *J. Electrocardiol.*, vol. 37, pp. 289–296, 2004.

[23] T. Watanabe, M. Yamaki, H. Tachibana, I. Kubota, and H. Tomoike, "Decrease in the high-frequency QRS components depending on the local conduction delay," *Jpn. Circ. J.*, vol. 62, pp. 844–848, 1998.

[24] S. Abboud, O. Berenfeld, and D. Sadeh, "Simulation of high-resolution QRS complex using a ventricular model with a fractal conduction system," *Circ. Res.*, vol. 68, no. 6, pp. 1751–1760, 1991.

[25] E. Pueyo, A. Arciniega, and P. Laguna, "High-frequency signature of the QRS complex across ischemia quantified by QRS slopes," in *Proc. Computers Cardiology*. CA: IEEE Comput. Soc. Press, 2005, pp. 659–662.

[26] G. Dori, A. Rosenthal, S. Fishman, Y. Denekamp, B. S. Lewis, and H. Bitterman, "Changes in the slope of the first major deflection of the ECG complex during acute coronary occlusion," *Comput. Biol. Med.*, vol. 35, no. 4, pp. 299–309, 2005.

[27] J. Pettersson, P. Lander, O. Pahlm, L. Sörnmo, S. Warren, and G. Wagner, "Electrocardiographic changes during prolonged artery occlusion in man: Comparison of standard and high-frequency recordings," *Clin. Physiol.*, vol. 18, pp. 179–186, 1998.

Esther Pueyo received the M.S. degree in mathematics and the Ph.D. degree in biomedical engineering from the University of Zaragoza, Zaragoza, Spain, in 1999 and 2006, respectively, where she is currently pursuing the Ph.D. degree in electronic engineering and communications.

During 2000, she was a Research Student at the Department of Mathematics, University of Zaragoza, where she developed a minor thesis in the field of calculus. Currently, she is an Assistant Professor at the same department. Her research interest is in the field of biomedical signal processing and her primary interest includes the study of the electrocardiographic signal.

Leif Sörnmo (SM'02) received the M.Sc. and Ph.D. degrees in electrical engineering from Lund University, Lund, Sweden, in 1978 and 1984, respectively.

He held a research position at the Department of Clinical Physiology, Lund University, from 1983 to 1995, where he worked on computer-based ECG analysis. Since 1990, he has been with the Signal Processing Group, Department of Electroscience, Lund University, where he is a Professor in biomedical signal processing. His main research interests include statistical signal processing and modeling of biomedical signals. Current research projects include methods for atrial fibrillation analysis, multimodal signal processing in hemodialysis, detection of otoacoustic emissions, and power-efficient signal processing in implantable devices. He is coauthor of *Bioelectrical Signal Processing in Cardiac and Neurological Applications* (Elsevier, 2005).

Dr. Sörnmo was Associate Editor of *Computers in Biomedical Research* from 1997 to 2000. He is currently Associate Editor of the IEEE TRANSACTIONS ON BIOMEDICAL ENGINEERING, and on the editorial boards of the *Journal of Electrocardiology*, and *Medical and Biological Engineering & Computing*.

Pablo Laguna (SM'06) was born in Jaca, Spain, in 1962. He received the M.S. degree in physics and the Ph.D. degree in physic science from the Science Faculty at the University of Zaragoza, Zaragoza, Spain, in 1985 and 1990, respectively.

Currently, he is Full Professor of Signal Processing and Communications in the Department of Electrical Engineering at the Engineering School, and a Researcher at the Aragón Institute for Engineering Research (I3A), both at the University of Zaragoza. From 1992 to 2005, he was an Associate Professor at the same university and from 1987 to 1992, he was an Assistant Professor of Automatic Control in the Department of Control Engineering at the Politecnic University of Catalonia (U.P.C.), Barcelona, Spain, and a Researcher in the Biomedical Engineering Division of the Institute of Cybernetics at U.P.C.–C.S.I.C. His professional research interests are in signal processing, in particular with biomedical applications. He is coauthor of the book *Bioelectrical Signal Processing in Cardiac and Neurological Applications* (Elsevier, 2005)